Arc Lavas on Both Sides of a Trench: 2 Triple-Junction Magmatism at the New Georgia Arc, Solomon Islands.

Article *in* Earth and Planetary Sciences Letters · January 2009

7 authors, including:

John Chadwick
College of Charleston
44 PUBLICATIONS **690** CITATIONS
SEE PROFILE

Michael Perfit
University of Florida
252 PUBLICATIONS **7,089** CITATIONS
SEE PROFILE

Brent I. A. Mcinnes
Curtin University
83 PUBLICATIONS **1,493** CITATIONS
SEE PROFILE

George D. Kamenov
University of Florida
147 PUBLICATIONS **1,859** CITATIONS
SEE PROFILE

Earth and Planetary Science Letters 279 (2009) 293–302

Contents lists available at ScienceDirect

Earth and Planetary Science Letters

journal homepage: www.elsevier.com/locate/epsl

Arc lavas on both sides of a trench: Slab window effects at the Solomon Islands triple junction, SW Pacific

John Chadwick [a,*], Michael Perfit [b], Brent McInnes [c], George Kamenov [b], Terry Plank [d], Ian Jonasson [e], Claire Chadwick [a]

[a] Dept. of Geography and Earth Sciences, University of North Carolina, Charlotte, USA
[b] Dept. of Geological Sciences, University of Florida, Gainesville, FL, USA
[c] CSIRO Exploration and Mining, Bentley, Western Australia, Australia
[d] Lamont-Doherty Earth Observatory, Division of Geochemistry, Palisades, NY, USA
[e] Geological Survey of Canada, Ottawa, ON, Canada K1A0E8

ARTICLE INFO

Article history:
Received 19 August 2008
Received in revised form 19 December 2008
Accepted 5 January 2009
Available online 29 January 2009

Editor: R.W. Carlson

Keywords:
Solomon Islands
Woodlark Spreading Center
triple junction
slab window
magma mixing
subduction
island arc

ABSTRACT

The Woodlark Spreading Center (WSC) is subducted at the San Cristobal trench, forming a triple junction at the New Georgia Group (NGG) arc in the Solomon Islands. WSC lavas are N-MORB at >100 km from the trench, but with decreasing distance they have increasingly arc-like Sr–Nd–Pb isotopic ratios, enrichments in Rb>K>Pb>Sr, and depletions in HFSE and Y. Within 50 km of the trench on the Simbo and Ghizo Ridges, many recovered samples are island arc tholeiites to medium-K calc-alkaline andesites and dacites, and many have the same or similar major and trace element and isotopic characteristics as true arc lavas in the NGG on the other side of the trench. Previous investigations have concluded that these WSC lavas are the result of relic back arc mantle enrichments resulting from subduction of the Pacific plate prior to the late Miocene at the North Solomon trench, >200 km to the north. However, the high-silica WSC lavas are more arc-like than those recovered from other distal back arcs, and are more voluminous, forming large submarine ridges and stratovolcanoes. We suggest that true arc mantle migrates across the plate boundary from the adjacent NGG arc through slab windows created by the subduction of the WSC. This leads to variable mixing between NGG arc and WSC N-MORB end-members, forming the transitional lavas recovered from the WSC. Lavas with similar arc-like characteristics have previously been recovered on the Chile Rise near where it is subducted at the Chile Trench, raising the possibility that such mantle transfer is a common phenomenon where active spreading centers are subducted. The presence of slab windows may also be responsible for the unusual forearc volcanism in the NGG, and melting of slab window margins may account for the presence of high-silica adakite-like lavas on the WSC.

1. Introduction

The triple junction formed by the Woodlark Spreading Center (WSC) and San Cristobal trench at the New Georgia arc of the Solomon Islands is the only location on Earth where an active or recently-active spreading ridge system and young oceanic crust are being subducted beneath an intra-oceanic arc. The triple junction area has several notable geological features, including abundant high-Mg picrites erupted in the arc (Ramsay et al., 1984; Schuth et al., 2004), forearc volcanism occurring only 30–40 km from the trench (Johnson and Tuni, 1987), and a rapidly uplifting forearc (Hughes et al., 1986; Mann et al., 1998; Taylor et al., 2005).

The focus of this study is the enigmatic arc-like chemistry of lavas erupted on the WSC near the triple junction, an apparent juxtaposition of spreading ridge tectonic and arc chemical regimes. Samples recovered on the ridge >100 km from the trench exhibit normal mid-ocean ridge basalt (N-MORB) chemistry, but with decreasing distance from the trench they are progressively more arc-like, a geographic trend first recognized following the 1982 cruise of the RV Kana Keoki (Johnson et al., 1987; Perfit et al., 1987; Trull et al., 1990). Some rocks recovered from <50 km from the trench on the Simbo and Ghizo Ridges (Fig. 1) are high-silica calc-alkaline rocks with arc-like geochemical characteristics that are indistinguishable from New Georgia Group (NGG) arc rocks on the other side of the trench. Previous research has concluded that this phenomenon is a result of relic back arc enrichment of the regional mantle by the Pacific slab (Johnson et al., 1987; Perfit et al., 1987), which subducted beneath the northern Solomon arc from the northeast prior to the late Miocene. We suggest an alternative explanation: that the subduction of the active WSC has led to the formation of slab windows that allow NGG arc mantle to flow across the convergent boundary to be tapped by the spreading ridge.

* Corresponding author. Tel.: +1 704 687 5947; fax: +1 704 687 5966.
E-mail address: djchadwi@uncc.edu (J. Chadwick).

0012-821X/$ – see front matter © 2009 Elsevier B.V. All rights reserved.
doi:10.1016/j.epsl.2009.01.001

2. Regional geology

2.1. Woodlark Spreading Center

The WSC is a 500-km-long, intermediate-rate (7.2 cm/yr) spreading ridge (Taylor, 1987). The system is divided into a series of E–W-trending first-order segments, which have a deep axial rift morphology that is typical of slow- to moderate-rate ridges, and are offset by N–S-trending transforms (Fig. 1). The segments are sub-divided into second-order segments that are rotated with respect to the trend of the first-order segments, as a result of synchronous counterclockwise rotation in spreading direction of up to 22° that occurred at 80 ka (Goodliffe et al., 1997). Spreading on the WSC began at about 5 Ma (Taylor, 1987; Mann, 1997) and has propagated to the west toward Papua New Guinea, creating the roughly triangular Woodlark Basin (Fig. 1, inset).

In the triple junction area, the morphology of the WSC system changes dramatically. Ghizo and Simbo Ridges are high-standing bathymetric features that are heavily dissected by NE–SW-oriented arcuate faults. Simbo Transform is the active WSC tectonic feature in contact with the trench, creating a trench–trench-transform triple junction between the Pacific, Australian, and Solomon Sea Plates (Taylor, 1987; Crook and Taylor, 1994). Simbo Ridge is a complex volcanic edifice that has formed along the east side of the 'leaky' Simbo Transform. The ridge rises nearly 2 km above the local basin floor, and shoals above sea level near where it contacts the trench to form volcanically-active Simbo Island. Ghizo Ridge is a southeastern bifurcation from Simbo Ridge, dominated on its eastern side by two large, morphologically young submarine stratovolcanoes; Kana Keoki and Coleman Seamounts, which are >10 km in diameter at their base and rise 2.3 and 2.8 km above the local seafloor, respectively. Taylor (1987) suggested that Ghizo Ridge was a former WSC spreading segment that was deformed and ceased spreading as it collided with the trench. Mann and others (1998) concluded that mechanical resistance due to subducting the rugged ridges may have terminated spreading on Ghizo Ridge and converted it to a strike–slip fault zone. Crook and Taylor (1994) suggested that Ghizo Ridge formed primarily as a result of differential uplift and shearing of fault blocks in the Woodlark Basin due to the plate collision and was never a WSC segment.

Subduction and volcanism in the New Georgia arc initiated in the late Miocene (6–8 Ma) in response to a major tectonic reorientation in the southwest Pacific (Karig and Mammerickx, 1972; Johnson et al., 1987). Prior to this time, the Pacific Plate had been subducting at the North Solomon (or Kilinailau–Vitiaz) trench (Fig. 1, inset), creating parts of the northern chain of islands in the Solomon arc. At 20–25 Ma, the >30-km-thick crust of the Ontong–Java Plateau began colliding with the North Solomon Trench (Petterson et al., 1997; 1999), and by the mid-Miocene, it had stifled Pacific and Australian plate convergence. Continued NE–SW compression was then accommodated by a reversal of arc polarity, and the current NE-directed subduction at the San Cristobal–New Britain trench system was initiated (Cooper and Taylor, 1985; Solomon, 1990).

2.2. New Georgia Group

The Solomon Islands are a collage of crustal terranes with discrete and complex histories (Coleman, 1966; Petterson et al., 1997) which form a NW–SE-trending double chain composed of Choiseul, Santa Isabel, Malaita (northern chain), and Guadalcanal, Makira, and the NGG (southern chain). The Miocene-recent NGG is itself composed of five large islands and a retinue of dozens of smaller islands and seamounts, which can be subdivided into two major physiographic groups with contrasting geology (Johnson et al., 1987). The 'main group' consists of the largest volcanic islands (Vella Lavella, Kolombangara, New Georgia, and Vangunu), with coalesced volcanic

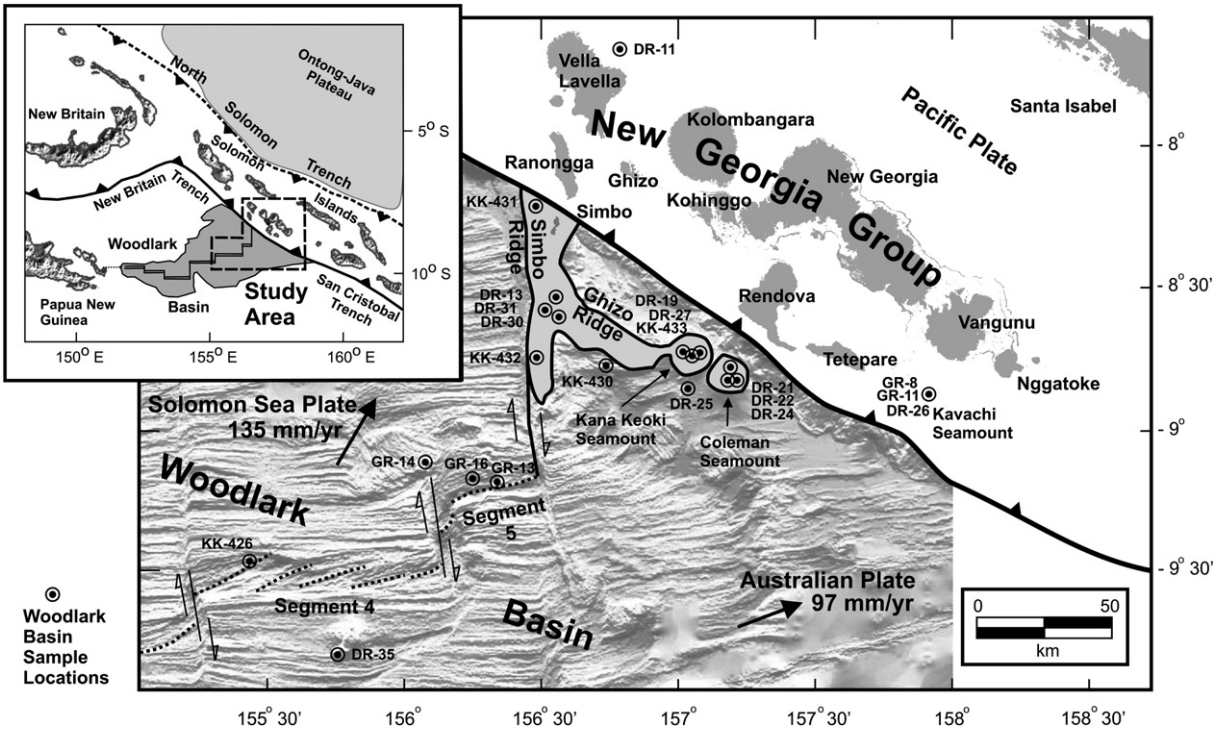

Fig. 1. The triple junction region between the Solomon Sea, Australian, and Pacific Plates, where the Woodlark Basin and Woodlark Spreading Center are subducted beneath the New Georgia Group of the Solomon Islands. Subduction was initiated here after it ceased on the North Solomon Trench due to the impingement of the Ontong-Java Plateau (inset). Rock samples collected in the New Georgia arc and Woodlark Basin for this study are shown (DR- and GR-), and the locations of additional Woodlark Basin samples collected during the 1982 Kana Keoki cruise (KK-) and used in this study are included. Bathymetry courtesy A. Goodliffe, and second-order ridge segment locations generalized from Goodliffe et al. (1997). Solomon Sea/Pacific and Australian/Pacific relative plate velocities are from Mann et al. (1998).

centers that are 45–75 km from the trench axis. The 'outer group' of smaller islands (Ranongga, Tetepare, and Rendova) are only 25–35 km from the trench in the forearc region. These islands consist mostly of submarine clastic rocks and coral platforms that have been uplifted as much as 1200 m. Rates of Holocene uplift in the forearc ranged up to 7.5–8.0 mm/a (Hughes et al., 1986; Mann et al., 1998; Taylor et al., 2005). During the 2007 M 8.1 Solomon Islands earthquake alone, coral reefs on the southern side of Ranongga Island were uplifted over 3 m (Albert et al., 2007; McAdoo et al., 2008).

The uplifted forearc islands correspond closely with Woodlark Basin bathymetric features that are in the process of being subducted and may be strongly coupled to the overlying plate (Mann et al., 1998); Ranongga and Ghizo Islands lie just across the trench from Simbo Ridge, and Rendova and Tetepare are across from Kana Keoki and Coleman Seamounts (Fig. 1). Indeed, projections of the trends of Simbo and Ghizo Ridges across the trench define the western and eastern limits of the NGG, respectively (Fig. 1), suggesting a strong connection between WSC subduction and NGG arc magmatism as well as forearc uplift (Johnson et al., 1987).

Beyond the boundaries of the Woodlark Basin, where older Australian and Solomon Sea plate oceanic crust is subducted, trenches are well-defined bathymetric features with depths ranging up to 7500 to 9000 m and Wadati–Benioff zones are clearly defined (Cooper and Taylor, 1987). Where the young lithosphere of the Woodlark Basin is subducted, particularly in the triple junction region, the San Cristobal trench is a poorly defined feature and shallows to depths of between 2500 to 5000 m. The Wadati–Benioff zone is diffuse here and dips at 30°–45°, with most earthquakes occurring at shallow depths <60–75 km (Weissel et al., 1982; Mann et al., 1998; Yoneshima et al., 2005). The absence of a deep trench and the lack of a clear Wadati–Benioff zone associated with subduction of the Woodlark Basin suggests that the young, buoyant lithosphere and impingement of the high-standing Simbo and Ghizo Ridges may be impeding subduction in the area, forming a pseudo-collisional boundary rather than a true trench (Mann et al., 1998).

The forearc outer group also includes Kavachi seamount, which has built small temporary islands at least seven times since the 1950's (Johnson and Tuni, 1987) and is located only about 30 km from the trench. During sampling for this study in 2000, Kavachi's summit was only tens of m below sea level and produced phreatomagmatic eruptions about every 5–7 min that rose up to 70 m above the ocean (Baker et al., 2002). Volcanoes on Rendova Island are also part of the forearc outer group, lying within 40 km of the trench. Other small seamounts, both active and dormant, have been reported in the near-trench forearc region as well, near Kavachi and to the west of Rendova (e.g. Cook Volcano).

3. Sample collection and geochemical analysis

Most of the rock samples analyzed in this study were collected during the May, 2000 cruise of Australia's Commonwealth Scientific and Industrial Research Organization (CSIRO) RV Franklin (FR04/00; 'Submarine, Hydrothermally Active Arc Volcanoes; 'SHAARC'; http://www.marine.csiro.au/nationalfacility/franklin/plans/2001/fr04_00's.html). Samples were collected from the WSC (Segments 4 and 5) and Woodlark Basin and in the NGG (including Kavachi) using dredges and rock-grab equipment (GPS sample locations in Table 1 and Fig. 1). Dredges were deployed and dragged by the ship over the ocean floor typically for a distance of 0.5 to 1 km, and successful hauls contained up to ~100 kg of rock. Successful rock grabs performed on the WSC recovered 5–50 g.

Representative samples of different rock types from each haul were distributed to the University of Florida, CSIRO, and the Australian National University. Additional submarine samples and geochemical data used in this study were recovered primarily during the 1982 RV Kana Keoki cruise (Perfit et al., 1987; sample numbers denoted with 'KK' are from this cruise.). Additional geochemical data from previous studies plotted in figures in this paper were obtained from the literature and unpublished data (Perfit et al., 1987; Johnson et al., 1987; Staudigel et al., 1987; Trull et al., 1990; Kamenov, 2004; Schuth et al., 2004; König et al., 2007; M. Perfit unpublished data) and the Petrological Database of the Ocean Floor (PetDB; http://www.petdb.org/petdbWeb/index.jsp).

Table 1
SHAARC sample locations

Sample	Location	Latitude	Longitude	Distance to trench (km)
Woodlark spreading center samples				
DR-35	Segment 4	−9.741	155.772	180.11
GR-14	Segment 5	−9.142	156.017	112.38
GR-16	Segment 5	−9.201	156.233	101.76
GR13	Segment 5	−9.220	156.317	97.74
Simbo and Ghizo Ridge samples				
DR-31	Simbo Ridge	−8.583	156.498	31.06
DR30	Simbo Ridge	−8.606	156.546	29.32
DR-13-1	Simbo Ridge	−8.542	156.540	24.60
DR25	Kana Keoki Smt.	−8.872	157.016	23.76
DR-21-2	Coleman Smt.	−8.841	157.159	13.71
DR22-1	Coleman Smt.	−8.842	157.189	12.43
DR27-2	Kana Keoki Smt.	−8.737	157.001	11.42
DR19-1	Kana Keoki Smt.	−8.750	157.029	11.17
DR24-1	Coleman Smt.	−8.795	157.172	8.52
New Georgia Arc Samples				
DR11-1A	NE of Vella Lavella	−7.513	156.661	–
DR26-2	Kavachi Smt.	−9.007	157.984	–
GR8	Kavachi Smt.	−9.006	157.980	–
GR11-2	Kavachi Smt.	−8.985	157.979	–

Samples are sorted by tectonic province and distance from the San Cristobal trench.

All SHAARC samples were crushed in a steel jaw crusher and, although nearly all were relatively fresh, the chips were then hand picked to remove any with obvious alteration. The remaining chips were cleaned with dilute HCL and rinsed with 2× de-ionized water. Samples to be analyzed by ICP-MS and XRF were further powdered in an agate mill. XRF spectrometry for some trace elements was performed on 5 g of powder mixed with 2.5 mL binder solution and compressed at 200 MPa. For ICP-MS analyses of a more complete suite of major and trace elements, 0.05 g of sample powder was dissolved in 3 mL HNO_3 and 1 mL HF, dried down and re-dissolved in 3 mL HNO_3 and 3 mL de-ionized water, and finally diluted by 1500 times with de-ionized water and analyzed at both the Geological Survey of Canada and Boston University (see Kelley et al., 2003 for methods). Sr, Nd, and Pb isotopic ratios were measured at the University of Florida Department of Geological Sciences using a "Nu-Plasma" multiple-collector inductively-coupled-plasma mass spectrometer (MC-ICP-MS), following methods described in Kamenov et al. (2008). The data reported are relative to the following long-term standard values: NBS 987 $^{87}Sr/^{86}Sr = 0.71025$ (+/−0.00003, 2σ), JNdi-1 $^{143}Nd/^{144}Nd = 0.512107$ (+/−0.000021, 2σ; which corresponds to 0.511846 for LaJolla), and NBS 981 $^{206}Pb/^{204}Pb = 16.937$ (+/−0.004, 2σ), $^{207}Pb/^{204}Pb = 15.490$ (+/−0.003, 2σ), and $^{208}Pb/^{204}Pb = 36.695$ (+/−0.009, 2σ). Over a three-year period, blank values ranged from 40 to 118 pg for Sr, 5 to 67 pg for Nd, and 4 to 56 pg for Pb isotopes.

4. Petrography and geochemical results

4.1. Woodlark Spreading Center

Following the RV Kana Keoki cruise in 1982, Perfit et al. (1987) and Johnson et al. (1987) noted a progressive change in chemical composition along the WSC. The additional samples collected and analyzed for this new study confirm and better characterize the

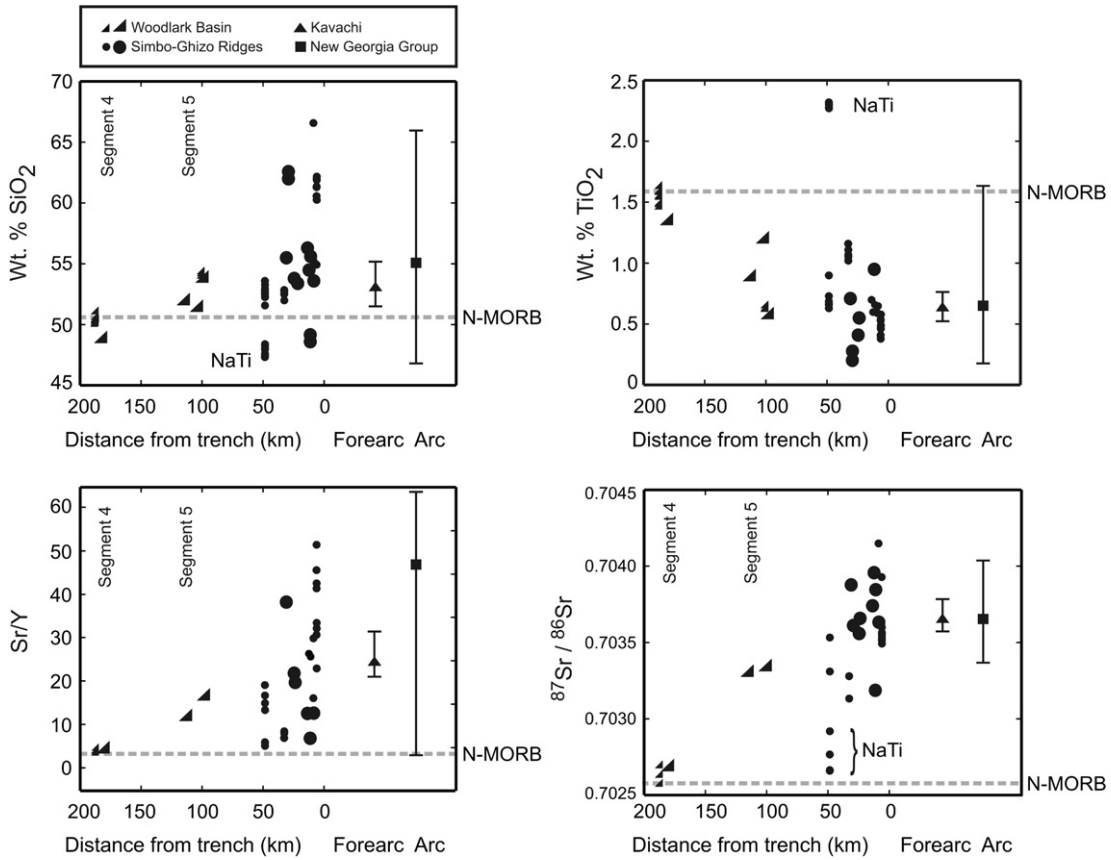

Fig. 2. Lavas from >150 km from the trench on Woodlark Segment 4 are N-MORB-like, but Segment 5 lavas, recovered about 100 km from the trench, are significantly more enriched and evolved with arc-like affinities. Many rocks recovered from the Simbo and Ghizo Ridges, <50 km from the trench, are petrographically and geochemically very similar to samples recovered from the New Georgia arc. See Section 2 of text for descriptions of Kavachi seamount in the forearc and Section 4.2 for a description of the unusual 'NaTi' basalts recovered from Simbo Ridge. Larger symbols denote SHAARC samples collected and analyzed for this study; small symbols and fields shown in Figs. 3–5 represent data from the literature (see Section 3 in text for references).

trends, which are observed in all of the major and trace elements and Sr–Nd–Pb isotopic ratios analyzed (Fig. 2).

Rock samples recovered from on and near WSC segment 4, acquired from two dredges (KK-426 and DR-35) about 180 km from the trench (Fig. 1), have major and trace element characteristics typical of N-MORB, including relatively low total alkalis (Fig. 3), low incompatible trace element concentrations and ratios (e.g. Sr/Y<4.75, K_2O/TiO_2<0.12), and depleted rare earth element (REE) signatures (La_N/Yb_N<0.75; Fig. 3). Sr–Nd–Pb isotopic ratios for segment 4 are also consistent with N-MORB (Table 2).

Samples from on and near segment 5 (the 1st active segment about 100 km from the triple junction) reveal clear chemical differences from the more distal segment 4. They have generally higher SiO_2 (including basaltic andesites) and Al_2O_3 and lower MgO and TiO_2, and some trace element concentrations and ratios are distinct from N-MORB (e.g. Sr/Y up to 16.3, K_2O/TiO_2 up to 0.76). Two samples (GR-13 and GR-14) have selective enrichments in large-ion lithophile element (LILE) concentrations and depletions in high field strength element (HFSE) concentrations relative to N-MORB (Fig. 4) that presumably reflect a slab component. They have flat to slightly enriched REE trends (La_N/Yb_N up to 2.05), and their REE and trace element patterns cross those of the Segment 4 N-MORB (Fig. 4), indicating that the magmas on Segment 4 and 5 are unlikely to have been derived from the same sources. Segment 5 samples also have significantly higher Sr and lower Nd isotopic ratios than Segment 4, and have Pb isotopic ratios that overlap with NGG arc lavas (Fig. 5), confirming that the lavas from the two segments are not related by differentiation of the same parent. Segment 5 has lavas with geochemical characteristics that are more similar to back arc basin basalts (BABB) or island arc tholeiites (IAT) than the N-MORB expected in this tectonic setting.

4.2. Simbo and Ghizo Ridges

Although Simbo and Ghizo Ridges are part of the Woodlark Basin in a geographic and tectonic sense, very few of the samples recovered there have N-MORB chemical and petrographic characteristics, and most reveal a strong influence of an arc component. Rocks recovered from these ridges (including Coleman and Kana Keoki Seamounts and Simbo Island; Fig. 1), from <50 km from the trench, range from basalts to dacites and generally follow a lower-alkali differentiation trend than those from the NGG arc, although there is significant overlap (Fig. 3). Rock types include porphyritic basalts containing abundant (15–20 vol.%) and large (up to 1 cm) clinopyroxene phenocrysts and lesser amounts (<5 vol.%) of olivine and plagioclase (ankaramites). Plagioclase- and/or pyroxene-rich basalts and andesites, and vesicular (>50% by volume) dacites (most from Kana Keoki Seamount) that contain amphibole and plagioclase were also recovered.

The geochemical characteristics of some Simbo and Ghizo lavas are similar to or indistinguishable from arc lavas in the NGG (Figs. 2–5). They have selective enrichments in LILE and depletions in HFSE and HREE relative to N-MORB (e.g. K_2O/TiO_2 up to 3.92; La_N/Yb_N up to 8.56; Sr/Y up to 51.4). Many of the most enriched Simbo and Ghizo Ridge lavas were recovered on the northern Simbo Ridge and Simbo Island (M. Perfit unpublished data; König et al., 2007) directly adjacent to the trench, and lavas become generally more depleted along the ridges

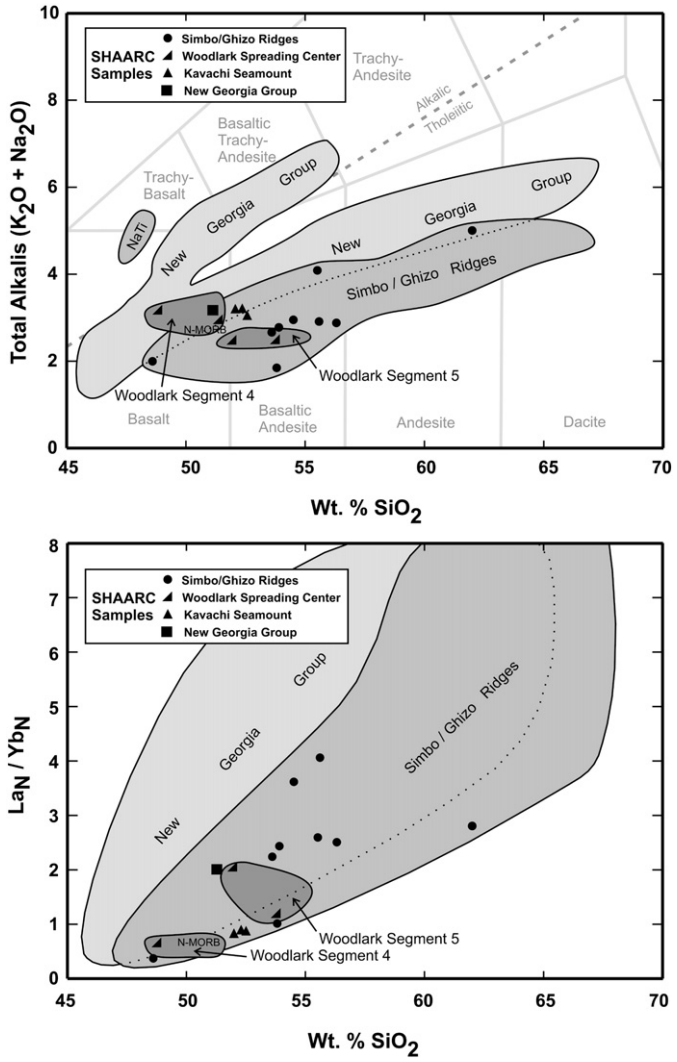

Fig. 3. Covariation of SiO_2 (wt.%) with total alkalis (wt.%) and La/Yb. Lavas from the Simbo and Ghizo Ridges range from basalts to dacites and have generally lower alkalis and REE enrichment than the New Georgia lavas for a given SiO_2, although there is significant overlap. Woodlark Segment 4 lavas are MORB-like and have higher alkalis but generally lower incompatible trace element enrichments than those from Segment 5. Symbols denote data from this study; outlined fields show ranges of data from the literature.

with distance from this area. Sr–Nd–Pb isotopic compositional ranges for most Simbo and Ghizo Ridge samples are distinct from N-MORB and are indistinguishable from NGG arc lavas, though some are transitional between WSC and NGG values (Fig. 5).

A few samples from the southern part of Simbo Ridge exhibit unusual geochemical patterns that are not typical of N-MORB, BABB, or arc lavas. These nepheline-normative trachybasalts are referred to as 'NaTi' basalts (Johnson et al., 1987; Perfit et al., 1987; Staudigel et al., 1987) for their unusually high Na_2O (>4.3 wt.%) and TiO_2 (>2.3 wt.%). They also have distinct enrichments in other moderately incompatible elements and HREE relative to other NGG and WSC lavas, and significant depletions in some of the more incompatible elements (Rb, Ba, K, Nb). They have the least radiogenic $^{87}Sr/^{86}Sr$ on Simbo and Ghizo Ridges (<0.703), with overall Sr–Nd–Pb isotopic characteristics that are similar to N-MORB from Woodlark segment 4 (Table 2 and Fig. 5). Their trace element patterns and rare earth element concentrations suggest that these basalts are the result of small extents of partial melting of a source that is highly depleted in the most incompatible elements (Perfit et al., 1987; Muenow et al., 1991).

4.3. New Georgia Group

Five major petrographic types have been identified in the NGG (Johnson et al., 1987), and basalts are the most widespread and voluminous (Ramsay et al., 1984; Schuth et al., 2004). Most abundant are arc ankaramites similar to those found on Simbo and Ghizo Ridges. Also found are basalts to basaltic andesites with large plagioclase phenocrysts (up to 1 cm), andesites to dacites containing plagioclase, hornblende, clinopyroxene, and minor orthopyroxene, and two-pyroxene andesites to dacites. Picrites with 15–40 vol.% olivine phenocrysts and 15–25 vol.% cpx and up to 29.6 wt.% MgO have also been recovered on New Georgia and Kohinggo Islands (Johnson et al., 1987; Ramsay et al., 1984; Schuth et al., 2004). Picrites are very rare in arc settings, and those from the New Georgia arc are the most magnesian lavas found so far in any active island arc system (Schuth et al., 2004).

Geochemical data from the literature show that NGG lavas fall into two groups on a total alkali vs. silica (TAS) diagram (Fig. 3); a lower-alkali group that ranges from high-Mg picrites to calc-alkaline dacites that overlaps with Simbo and Ghizo lavas, and a distinctly more alkaline group that includes trachybasalts to trachyandesites. The majority of NGG rocks have major and trace element characteristics that are typical of arcs, with enrichments in LILE and depletions in HFSE relative to N-MORB (Fig. 4). Most NGG lavas have moderately enriched REE signatures that are similar to the Simbo and Ghizo Ridges (La_N/Yb_N up to 8.87). Also like Simbo and Ghizo Ridges, HREE concentrations are low relative to N-MORB (Fig. 4) and there are negative correlations between LILE and HREE. Sr–Nd–Pb isotopic ratios from the NGG broadly overlap with ranges for Simbo and Ghizo Ridges as well as WSC Segment 5 (Figs. 2 and 5).

Although Kavachi Seamount is geographically part of the New Georgia Group, we discuss it separately due to its unusual position in the forearc (<30 km from the trench). All rocks recovered at Kavachi are basalts or basaltic andesites, and all are ankaramites with large (up to 1 cm) cpx similar to those found on the Simbo and Ghizo Ridges and in the NGG. The lavas are transitional arc tholeiite to calc-alkaline, with low total alkalis similar to Simbo and Ghizo values, flat REE signatures ($La_N/Yb_N \sim 1$), and arc-like enrichments in Sr, Pb, and K and depletions in HFSE. Sr–Nd–Pb isotopic compositions generally overlap those of the NGG and Simbo and Ghizo Ridges, although the Pb isotopic values are similar to the least radiogenic compositions from the NGG (Fig. 5).

5. Discussion

Previous studies concluded that the geographic trends in geochemistry and BABB- to arc-like lavas on the WSC are the result of long-lived back arc "conditioning" of the Woodlark Basin mantle by the Pacific slab (Johnson et al., 1987; Perfit et al., 1987; König et al., 2007), which subducted beneath the northern chain of the Solomon Islands from the northeast prior to the late Miocene (Fig. 1, inset). The geochemical enrichment of back arc basin lavas is commonly observed, with compositions that are typically intermediate between N-MORB and IAT (e.g. Sinton and Fryer, 1987; Taylor and Martinez, 2003; Pearce and Stern, 2006). BABB enrichments are generally hypothesized to be the result of arc components metasomatizing N-MORB mantle (Stern et al., 1990). It is reasonable to consider that the WSC, in a position that was formerly in the distal back arc area of the Pacific slab, could tap mantle that was previously metasomatized by back arc processes.

The arc-like lavas from Simbo and Ghizo Ridges and Segment 5 are erupted 200–250 km from the pre-Miocene North Solomon trench, in a far back arc position (Fig. 1 inset). It is not unusual for subtle back-arc enrichments to be observed at this distance (e.g. East Scotia Ridge; Fretzdorff et al., 2002), but IAT to calc-alkaline lavas with arc-like enrichments similar to those described above have only been observed in the immediate back arc region of other arcs, and the

Table 2
Major, trace element, and isotopic data for SHAARC samples

Sample	DR35	GR13	GR14	GR16	DR13-1	DR30	DR31	DR19-1	DR27-2	DR25	DR21-2	DR22-1	DR24-1	DR26-2	GR11-2	GR8	DR11-1
	Segment 4	Segment 5	Segment 5	Segment 5	Simbo Ridge	Simbo Ridge	Simbo Ridge	Ghizo Ridge	Ghizo Ridge	Ghizo Ridge	Ghizo Ridge	Ghizo Ridge	Ghizo Ridge	Kavachi Smt.	Kavachi Smt.	Kavachi Smt.	NGG
SiO_2	50.2	53.1	50.4	51.4	53.8	62.0	55.5	55.6	48.6	53.9	56.3	54.5	53.6	52.0	52.5	52.3	51.3
TiO_2	1.37	0.56	0.85	1.19	0.41	0.26	0.71	0.66	0.95	0.55	0.70	0.60	0.65	0.61	0.60	0.59	0.76
Al_2O_3	15.5	15.4	15.6	16.1	16.5	17.6	17.6	15.9	17.1	17.7	17.1	15.8	16.1	16.9	16.4	18.0	13.8
Fe_2O_3T	10.20	7.11	7.70	7.84	8.55	3.91	7.64	9.37	8.83	8.35	8.05	9.46	8.04	9.14	9.39	9.11	9.10
MnO	0.18	0.12	0.15	0.16	0.14	0.07	0.12	0.16	0.16	0.14	0.13	0.15	0.14	0.16	0.17	0.15	0.15
MgO	7.80	9.19	8.15	6.24	6.45	3.22	4.39	4.86	9.17	5.06	4.81	4.98	6.68	6.69	7.37	5.86	9.20
CaO	12.30	11.20	11.00	10.89	10.70	6.38	9.31	8.69	12.70	10.10	9.39	9.41	9.90	10.30	11.40	9.90	9.35
Na_2O	2.86	2.11	2.15	2.72	1.46	4.07	2.61	2.05	1.95	2.14	2.12	2.05	2.06	2.37	1.99	2.39	2.11
K_2O	0.14	0.32	0.55	0.23	0.39	0.94	1.48	0.86	0.05	0.64	0.76	0.90	0.61	0.83	0.78	0.82	0.93
P_2O_5	0.10	0.07	0.12	0.13	0.03	0.07	0.25	0.06	0.05	0.10	0.13	0.21	0.11	0.08	0.09	0.09	0.15
Total	100.7	99.2	96.7	96.9	98.4	98.5	99.6	98.2	99.5	98.7	99.5	98.1	97.9	99.1	100.7	99.2	96.8
Zr	94.6	44.4	61.1	–	16.9	56.4	54.8	60.6	46.3	34.2	45.6	44.1	44.5	30.6	28.9	32.8	61.4
Sr	142	232	217	–	240	476	589	417	129	309	258	434	233	319	311	345	495
Y	30.1	14.2	17.8	–	11.0	6.4	15.4	16.3	18.9	15.7	20.6	16.5	18.5	15.0	14.8	15.8	16.1
Rb	0.717	4.74	7.09	–	5.86	15.9	24.3	18.3	0.611	11.8	13.0	16.8	10.2	13.7	12.9	14.3	13.9
Nb	1.81	1.34	7.07	–	0.66	1.80	1.44	4.93	0.70	1.78	3.60	1.51	4.00	0.41	0.40	0.47	1.09
Ba	4.39	51.4	70.8	–	81.8	200	173	114	8.81	100	113	143	90.0	105	99.2	111	121
Pb	0.436	0.933	1.29	–	0.986	2.76	3.24	2.07	0.340	1.66	1.67	2.54	1.33	1.71	1.58	1.76	2.71
Cs	0.004	0.076	0.104	–	0.114	0.346	0.372	0.203	0.003	0.195	0.205	0.263	0.159	0.146	0.141	0.161	0.278
Hf	2.55	1.15	1.57	–	0.549	1.45	1.52	1.63	1.36	1.11	1.43	1.37	1.30	1.04	1.01	1.10	1.68
Cr	324	294	280	–	110	10.5	40.2	2.13	424	56.8	68.5	43.8	191	136	206	84	635
Ni	73.4	176	129	–	49.0	29.1	29.9	14.6	187	44.9	40.8	29.6	91.9	53.3	66.8	56.8	204
Sc	40.2	33.1	34.8	–	39.0	16.7	30.2	37.4	34.0	35.1	35.8	39.7	39.6	33.6	37.5	30.7	32.1
U	0.05	0.103	0.234	–	0.096	0.233	0.344	0.547	0.021	0.327	0.374	0.499	0.308	0.137	0.134	0.155	0.297
Th	0.087	0.244	0.587	–	0.224	0.465	0.752	1.49	0.091	0.919	1.06	1.31	0.850	0.310	0.296	0.353	0.898
Li	7.01	5.29	3.60	–	4.51	10.75	7.58	7.00	2.89	6.61	7.76	5.84	6.61	6.19	6.40	7.09	8.60
Be	0.528	0.359	0.552	–	0.218	0.630	0.810	0.677	0.202	0.326	0.429	0.538	0.404	0.291	0.264	0.270	0.576
V	244	217	247	–	270	151	334	321	228	323	324	378	322	300	315	318	230
Co	41.9	35.7	37.8	–	33.1	14.2	23.9	30.4	44.1	28.2	25.5	30.2	30.5	33.7	32.5	31.7	37.4
Cu	76.2	74.9	66.3	–	39.2	34.2	133.1	14.6	27.8	101.4	82.6	113.2	79.4	106.2	123.5	137.5	50.2
Ga	15.3	12.0	13.3	–	12.7	14.2	16.5	15.0	14.4	15.1	16.1	14.8	14.4	14.8	14.4	16.1	14.0
Zn	75.4	48.3	53.7	–	59.0	34.4	58.9	71.5	54.4	68.9	67.3	74.4	67.9	69.3	69.6	73.5	70.6
Ta	0.12	0.08	0.45	–	0.06	0.10	0.09	0.30	0.07	0.10	0.20	0.08	0.23	0.08	0.04	0.05	0.08
La	2.79	2.60	5.47	–	1.82	2.99	6.37	10.42	1.13	6.28	8.25	9.38	6.63	1.99	1.94	2.22	4.86
Ce	9.48	6.64	12.72	–	4.26	6.40	14.32	21.32	4.05	12.95	17.07	19.73	13.85	4.88	4.81	5.41	11.17
Pr	1.73	1.04	1.73	–	0.65	0.84	2.16	2.83	0.74	1.79	2.29	2.77	1.88	0.81	0.81	0.90	1.70
Nd	9.56	4.98	7.79	–	3.15	3.38	9.91	11.67	4.35	7.62	9.86	11.84	8.02	4.28	4.22	4.64	7.95
Sm	3.24	1.48	2.11	–	0.99	0.77	2.54	2.69	1.77	1.95	2.47	2.85	2.11	1.44	1.45	1.57	2.15
Eu	1.19	0.54	0.77	–	0.43	0.31	0.88	0.92	0.80	0.68	0.82	0.91	0.73	0.59	0.58	0.62	0.78
Gd	4.40	1.93	2.69	–	1.37	0.86	2.83	2.78	2.71	2.30	2.99	3.04	2.63	1.99	2.05	2.17	2.56
Tb	0.807	0.348	0.480	–	0.257	0.148	0.464	0.461	0.505	0.402	0.526	0.487	0.472	0.370	0.374	0.394	0.439
Dy	5.03	2.24	2.98	–	1.71	0.94	2.77	2.70	3.28	2.52	3.32	2.83	2.95	2.36	2.43	2.54	2.72
Ho	1.08	0.50	0.64	–	0.39	0.22	0.57	0.57	0.73	0.56	0.73	0.59	0.67	0.54	0.54	0.57	0.57
Er	3.05	1.44	1.82	–	1.13	0.66	1.64	1.66	2.05	1.64	2.14	1.71	1.92	1.56	1.56	1.63	1.64
Yb	2.88	1.47	1.78	–	1.20	0.79	1.64	1.71	1.99	1.72	2.20	1.73	1.98	1.60	1.59	1.70	1.61
Lu	0.447	0.231	0.281	–	0.191	0.131	0.259	0.273	0.302	0.273	0.353	0.275	0.314	0.253	0.250	0.267	0.254
$^{87/86}Sr$	0.70268	0.70335	0.70330	–	0.70356	0.70361	0.70388	0.70385	0.70319	0.70366	0.70374	0.70396	0.70363	0.70365	–	0.70370	–
$^{143/144}Nd$	0.513117	0.513075	0.513016	–	0.513013	0.513033	0.512978	0.512974	0.513118	0.513004	0.513019	0.512980	0.512991	0.513055	–	0.513036	–
$^{206/204}Pb$	18.184	18.416	18.527	–	18.486	18.465	18.449	18.474	18.340	18.484	18.484	18.457	18.467	18.385	–	18.380	–
$^{207/204}Pb$	15.463	15.502	15.536	–	15.514	15.513	15.515	15.519	15.494	15.515	15.515	15.517	15.511	15.508	–	15.506	–
$^{208/204}Pb$	37.787	38.128	38.297	–	38.247	38.228	38.197	38.236	38.023	38.222	38.228	38.216	38.212	38.184	–	38.179	–

Major elements and Ta by ICP-MS at Geological Survey of Canada; all other trace elements by ICP-MS at Boston University. Major elements for GR16 by electron microprobe, and isotopic data from the University of Florida.

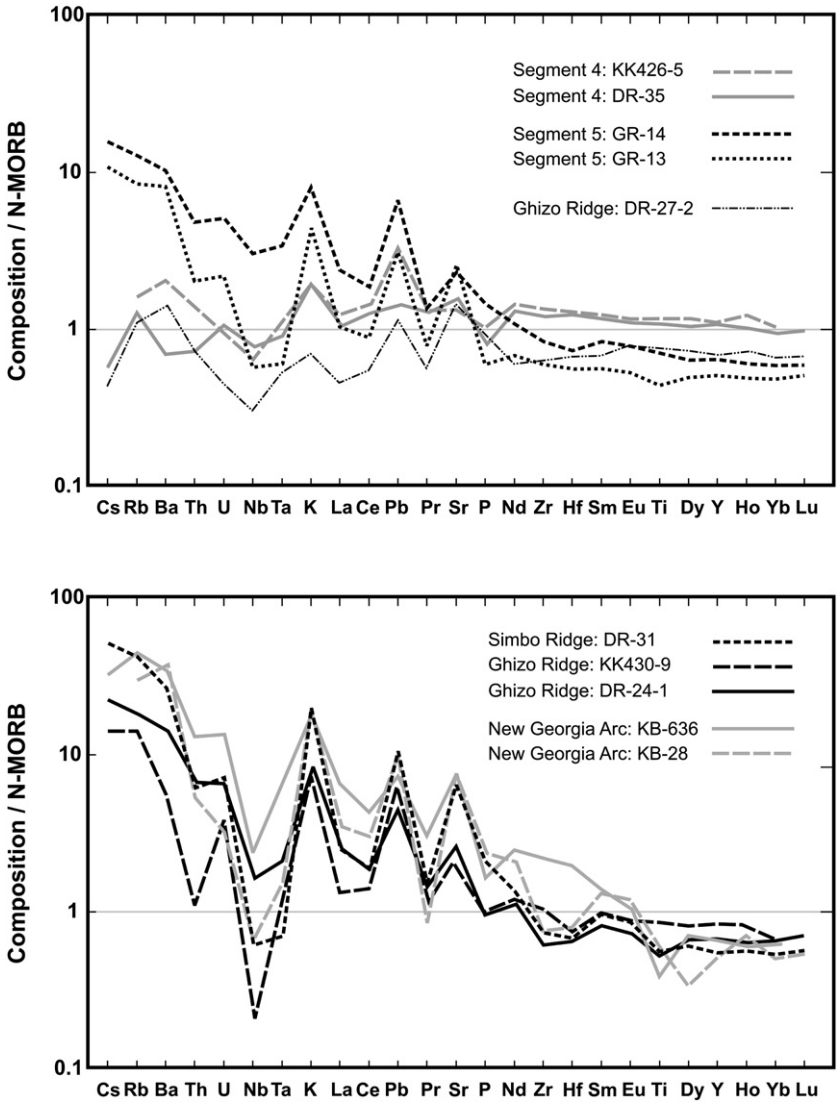

Fig. 4. MORB-normalized (Sun and McDonough, 1989) trace element patterns for typical samples from Woodlark Segments 4 and 5, Simbo and Ghizo Ridges, and the New Georgia arc. Lavas from Segment 4 have a typical depleted MORB-like pattern with minor enrichments in Pb and K, but Segment 5 and most Simbo/Ghizo lavas have arc-like enrichments in LILE, and depletions in the HFSE Nb and Ta relative to N-MORB.

magnitude of the arc component typically decreases with distance away from the trench (Sinton et al., 2003; Taylor and Martinez, 2003). The production of large andesite to dacite stratovolcanoes with fully arc-like major and trace element and isotopic enrichments have not been observed this far from the trench in any other back arc setting. If the subducted Pacific plate has any geochemical influence at this distance and >5 Ma after the subduction polarity reversal, it would be expected to be subtle and transitional, similar to that observed in other distal back arcs.

The geochemical data presented above indicate that some WSC Segment 5 and Simbo and Ghizo Ridge lavas from the Woodlark Basin have intermediate compositions between the N-MORB recovered from Segment 4 and NGG arc lavas, but some are essentially identical to typical NGG lavas. These strong geochemical similarities suggest that the lavas are derived from very similar arc mantle sources and are genetically related, despite the presence of the plate boundary between them.

Klein and Karsten (1995) identified arc-affinity lavas on Chile Ridge segments nearest to where it is subducted at the Chile Trench, and suggest that arc components may have been derived from the adjacent subduction zone. Though these Chile Ridge lavas are all basalts, they have arc-like trace element and isotopic characteristics that are similar to those recovered from the WSC, suggesting that a similar process is occurring at the two triple junctions that allows the transfer of arc mantle across the plate boundary.

5.1. Slab windows

In most arc settings, subducted oceanic lithosphere is old and thick and presents an impenetrable barrier to the exchange of asthenosphere between the two adjacent plates. The portions of the upper mantle on either side of the trench are isolated from one another and typically have very different geochemical histories. When a spreading ridge system is subducted, however, the diverging plates may continue to separate without crust production, opening an asthenosphere-filled gap called a slab window (Dickinson and Snyder, 1979; Thorkelson, 1996; Thorkelson and Breitsprecher, 2005). Although the triple junction in this study is currently a trench–trench-transform variety, previously subducted ridge segments may have formed slab windows that provide conduits for arc mantle from beneath the NGG to migrate across the plate boundary and be tapped by the WSC

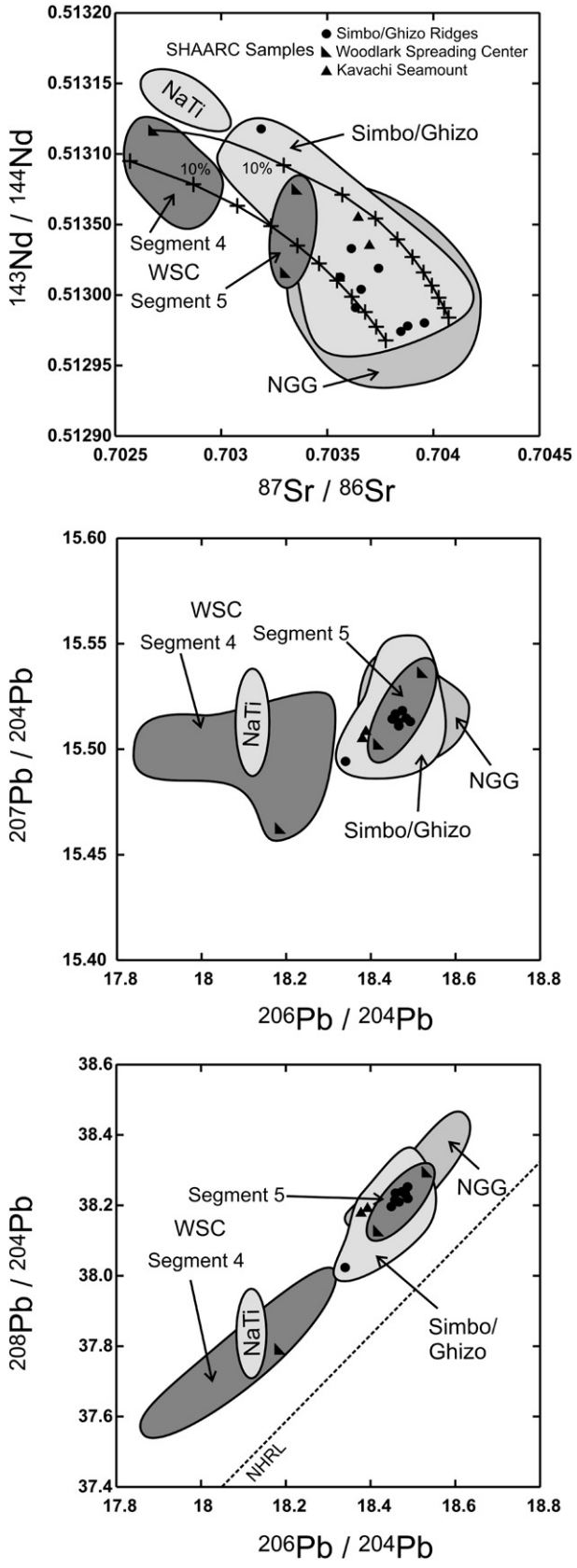

Fig. 5. Sr, Nd, and Pb isotopic ratios show general overlap between New Georgia, Simbo/Ghizo, and Segment 5 lavas in all isotopic systems. Mixing between Segment 4 MORB and more radiogenic New Georgia end-members (top) is consistent with the variations of Simbo/Ghizo and Segment 5 compositions, suggesting that mixing between arc and MORB components is occurring to produce the intermediate lavas.

(Fig. 6). Magnetic data suggest that at least three segments have been subducted since the initiation of Woodlark Basin subduction (Taylor, 1987).

Klein and Karsten (1995) suggested that slab windows may provide an avenue of communication between the sub-arc mantle and the adjacent Chile Rise as one possible explanation for the arc-affinity lavas they observed there. Mantle flow through a slab window formed by the subducted Cocos–Nazca ridge has similarly been invoked by Johnston and Thorkelson (1997) to explain the presence of Galapagos plume geochemical characteristics in lavas on the Caribbean plate.

A scenario involving mantle flow through Woodlark slab windows is consistent with Simbo Ridge magmatism that has been most productive and arc-like where it is in contact with the trench at Simbo Island and decreases with distance from the trench along the WSC. If arc mantle is sourced from the NGG side of the slab and mixes with Woodlark N-MORB, it is expected that its geochemical influence would be highest in the immediate vicinity of the trench and gradually diminish with distance from the arc as observed (Fig. 2). Fig. 5 shows the results of linear mixing analyses between NGG and WSC N-MORB end-members in Sr–Nd isotopic space. The results show that Segment 5 lavas have between 10 and 40% of the arc component, and that most Simbo and Ghizo Ridge lavas are dominated by it.

Ridge subduction and the formation of slab windows can also be invoked to explain the anomalous volcanism in the NGG forearc, a region that is amagmatic in most arcs. Only 30–40 km from the trench, Kavachi seamount and other NGG forearc volcanoes likely have no significant mantle wedge beneath them. However, a narrow slab window passing closely beneath the thin forearc crust may result in the "blowtorch effect", wherein the subducted spreading axis results in a thermal anomaly, high degrees of partial melting, and volcanism (Marshak and Karig, 1977; Delong et al., 1979; Thorkelson and Breitsprecher, 2005). Slab windows are likely responsible for past magmatism at other Pacific rim forearcs where ridge subduction has occurred (e.g. Forsythe et al., 1986; Hibbard and Karig, 1990; Groome et al., 2003; Madsen et al., 2006), but the NGG is the only location on Earth where this phenomenon may be occurring today (Johnson et al., 1987). As slab windows are further subducted past the front of the overriding plate and forearc, they then encounter the mantle wedge and flow that can push arc-influenced mantle across the plate boundary to the Woodlark Basin side as described above (Fig. 6).

The subducted WSC and slab windows may also be responsible for the andesitic and dacitic lavas on Simbo and Ghizo Ridges. The presence of basalts with arc-like geochemical characteristics is readily explained by the transfer of slab-metasomatized NGG mantle beneath the Woodlark Basin. The generation of high-silica lavas, however, typically requires fractional crystallization, assimilation, and/or magma mixing in relatively thick arc crust (e.g. Defant and Nielson, 1990), which is not expected or apparent on the Woodlark Basin. Defant and Drummond (1990) proposed that young, relatively warm lithosphere near a subducted spreading ridge such as the WSC is susceptible to partial melting to form adakites; andesitic to dacitic melts with geochemical characteristics that are distinct from typical arc lavas. Thorkelson and Breitsprecher (2005) identified slab windows in particular as important sites for slab melting, suggesting that the thin lithosphere around the edges of slab windows are most likely to thermally equilibrate and partially melt. Further study is required to understand the importance of Woodlark slab melting and the generation of adakites in this triple junction area.

6. Conclusions

A major element, trace element, and isotopic study of rocks from the Woodlark Basin and New Georgia arc in the southwestern Pacific has revealed an unambiguous subduction component in lavas on the WSC near where it is subducted at the San Cristobal trench. These lavas

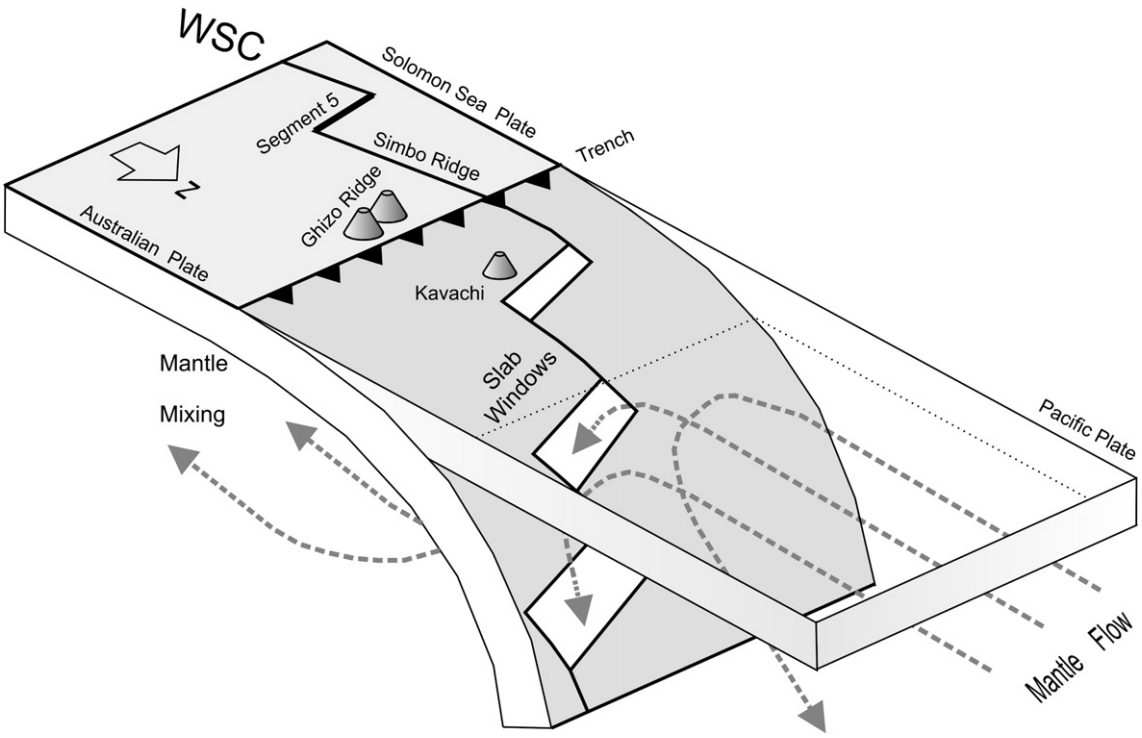

Fig. 6. Conceptual diagram of the triple junction region showing how flow in the sub-arc mantle wedge may force arc mantle through slab windows, allowing it to mix with MORB mantle beneath the Woodlark Spreading Center. Progressive dilution of the arc component with distance from the trench can explain the geochemical trends observed along the ridge (Fig. 2). Magnetic anomaly mapping (Taylor, 1987) suggest at least three short ridge segments have been subducted since the Woodlark Basin formed. Kavachi seamount probably has no mantle wedge beneath it, but the passage of a slab window beneath the forearc may induce volcanism here via the 'blowtorch effect' (Delong et al., 1979).

are selectively enriched in Rb>K>Pb>Sr and depleted in HFSE, with Sr–Nd–Pb isotopic compositions that are essentially the same as those of many NGG lavas. Some WSC Segment 5 and Simbo and Ghizo Ridge samples are intermediate between WSC N-MORB and arc compositions, consistent with mixing between the two components. Previous studies have concluded that the arc-like enrichments are due to relic back arc magmatic processes behind the North Solomon trench to the north, which ceased most subduction prior to the late Miocene polarity reversal that created the New Georgia arc and Woodlark Basin. We suggest that the great distance between the voluminous arc-affinity rocks on the WSC and the North Solomon trench and their proximity and chemical similarity to NGG arc lavas indicate that WSC lavas are a product of local Woodlark Basin subduction, despite their eruption on the "wrong" side of the trench. Slab windows created by subducted WSC ridge segments may allow flow beneath the NGG to push slab-metasomatized mantle across the plate boundary to be tapped by the WSC. Similar arc-affinity lavas have been recovered on the Chile Rise near its triple junction with the Chile trench, suggesting that this type of transfer of arc components is common where active ridges are subducted. Slab windows may also be responsible for volcanism in the NGG forearc, and partial melting of slab window margins may have lead to the high-silica, adakite-like lavas in the triple junction area.

Acknowledgments

The authors wish to thank the captain and crew of the RV Franklin for their support during sample collection. We also thank Linda Farr for her assistance with the ICP-MS analyses at Boston University, Peter Belanger and the Analytical Chemistry staff at the Geological Survey of Canada, and Ian Ridley for his electron microprobe analyses at the U.S. Geological Survey in Denver. We also thank EPSL editor Rick Carlson and reviewers Derek Thorkelson and Bob Stern for their very helpful comments on the manuscript. Field and laboratory investigations were supported by NSF grant # OCE-9403773 awarded to M. Perfit.

References

Albert, S., Udy, J., Baines, G., McDougall, D., 2007. Dramatic tectonic uplift of fringing reefs on Ranongga Is., Solomon Islands. Coral Reefs 26, 983.
Baker, E.T., Massoth, G.J., de Ronde, C.E.J., Lupton, J.E., Lebon, G., McInnes, B.I.A., 2002. Observations and sampling of an ongoing subsurface eruption of Kavachi volcano, Solomon Islands, May 2000. Geology 30, 975–978.
Coleman, P.J., 1966. The Solomon Islands as an island arc. Nature 211, 1249–1250.
Cooper, P.A., Taylor, B., 1985. Polarity reversal in the Solomon Islands arc. Nature 314, 428–430.
Cooper, P., Taylor, B., 1987. The spatial distribution of earthquakes, focal mechanisms, and subducted lithosphere in the Solomon Islands. In: Taylor, Exon (Eds.), Marine Geology, Geophysics, and Geochemistry of the Woodlark Basin — Solomon Islands. Circum-Pacific Council for Energy and Mineral Resources, vol. 7, pp. 67–88.
Crook, K.A., Taylor, B., 1994. Structure and Quaternary history of the Woodlark Triple Junction Region, Solomon Islands. Marine Geophys. Res. 16, 65–89.
Defant, M.J., Drummond, M.S., 1990. Derivation of some modern arc magmas by melting of young subducted lithosphere. Nature 347, 662–665.
Defant, M.J., Nielson, R.J., 1990. Interpretation of open system petrogenetic processes: phase equilibria constraints on magma evolution. Geochim. Cosmochim. Acta 54, 87–102.
Delong, S.E., Schwarz, W.M., Anderson, R.N., 1979. Thermal effects of ridge subduction. Earth Planet. Sci. Lett. 44, 239–246.
Dickinson, W.R., Snyder, W.S., 1979. Geometry of subducted slabs related to San Andreas transform. Journal of Geology 87, 609–627.
Forsythe, R.D., Nelson, E.P., Carr, M.J., Kaeding, M.E., Herve, M., Mpodozis, C., Soffia, J.M., Harambour, S., 1986. Pliocene near-trench magmatism in Southern Chile: a possible manifestation of ridge collision. Geology 14, 23–27.
Fretzdorff, S., Livermore, R.A., Devey, C.W., Leat, P.T., Stoffers, P., 2002. Petrogenesis of the back-arc East Scotia Ridge, South Atlantic Ocean. Journal of Petrology 43, 1435–1467.
Goodliffe, A.M., Taylor, B., Martinez, F., Hey, R.N., Maeda, K., Ohno, K., 1997. Synchronous reorientation of the Woodlark Basin spreading center. Earth Planet. Sci. Lett. 146, 233–242.
Groome, W.G., Thorkelson, D.J., Friedman, R.M., Mortenson, J.K., Massey, N.W.D., Marshall, D.D., Layer, P.W., 2003. Magmatic and tectonic history of the Leech River Complex, Vancouver Island, British Columbia: evidence for ridge-trench intersection and accretion of the Crescent Terrane. In: Sisson, V.B., Roeske, S.M., Pavlis, T.L. (Eds.), Geological Society of America Special Paper, vol. 371, pp. 327–353.
Hibbard, J.P., Karig, D.E., 1990. Structural and magmatic responses to spreading ridge subduction: an example from southwest Japan. Tectonics 9, 207–230.
Hughes, G.W., Varol, O., Dunkley, P.N., 1986. Pleistocene uplift of Tetepare Island, Solomon Group, as implied by foraminiferal and calcareous nanofossil Evidence. Proc. R. Soc. N. Bull. 24, 397–408.

Johnson, R.W., Tuni, D., 1987. Kavachi, an active forearc volcano in the western Solomon Islands: reported eruptions between 1950 and 1982, 1987. In: Taylor, Exon (Eds.), Marine Geology, Geophysics, and Geochemistry of the Woodlark Basin — Solomon Islands. Circum-Pacific Council for Energy and Mineral Resources, vol. 7, pp. 89–112.

Johnston, S.T., Thorkelson, D.J., 1997. Cocos–Nazca slab window beneath Central America. Earth Planet. Sci. Lett. 146, 465–474.

Johnson, R.W., Langmuir, C.H., Perfit, M.R., Staudigel, H., Dunkley, P.N., Chappell, B.W., Taylor, S.R., Baekisapa, M., 1987. Ridge subduction and forearc volcanism: petrology and geochemistry of rocks dredged from the western Solomon Arc and Woodlark Basin. In: Taylor, Exon (Eds.), Marine Geology, Geophysics, and Geochemistry of the Woodlark Basin — Solomon Islands. Circum-Pacific Council for Energy and Mineral Resources, vol. 7, pp. 113–154.

Kamenov, G.D., 2004. Magmatism and ore deposit formation in SW Pacific island arcs. Unpublished Ph.D. thesis, Department of Geological Sciences, University of Florida, 130pp.

Kamenov, G.D., Perfit, M.R., Mueller, P.A., Jonasson, I.R., 2008. Controls on magmatism in an island arc environment: study of lavas and sub-arc xenoliths from the Tabar–Lihir–Tanga–Feni island chain, Papua New Guinea. Contrib. Mineral. Petrol. 155, 635–656.

Karig, D.E., Mammerickx, J., 1972. Tectonic framework of the New Hebrides island arc system. Mar. Geol. 12, 187–205.

Kelley, K.A., Plank, T., Ludden, J.N., Staudigel, H., 2003. The composition of altered oceanic crust at ODP sites 801 and 1149. Geochem. Geophys. Geosyst. 4, 8910.

Klein, E.M., Karsten, J.L., 1995. Ocean-ridge basalts with convergent-margin geochemical affinities from the Chile ridge. Nature 374, 52–57.

König, S., Schuth, S., Munker, C., Qopoto, C., 2007. The role of slab melting in the petrogenesis of high-Mg andesites: evidence from Simbo Volcano, Solomon Islands, Contrib. Mineral. Petrol. 153, 85–103.

Madsen, J.K., Thorkelson, D.J., Friedman, R.M., Marshall, D.D., 2006. Cenozoic to Recent plate configurations in the Pacific Basin: ridge subduction and slab window magmatism in western North America. Geosphere 2, 11–34.

Mann, P., 1997. Model for the formation of large transtensional basins in zones of tectonic escape. Geology 25, 211–214.

Mann, P., Taylor, F.W., Lagoe, M.B., Quarles, A., Burr, G., 1998. Accelerating late Quaternary uplift of the New Georgia Island Group (Solomon Island Arc) in response to subduction of the recently active Woodlark Spreading Center and Coleman Seamount. Tectonophysics 295, 259–306.

Marshak, R.S., Karig, D.E., 1977. Triple junctions as a cause for anomalously near-trench igneous activity between the trench and volcanic arc. Geology 5, 233–236.

McAdoo, B.G., Fritz, H.M., Jackson, K.L., Kalligeris, N., Kruger, J., Bonte-Grapentin, M., Moore, A.L., Rafiau, W.B., Billy, D., Tiano, B., 2008. Solomon Islands tsunami, one year later. EOS, Trans. Amer. Geophys. Union 89, 169–170.

Muenow, D.W., Perfit, M.R., Aggrey, K.E., 1991. Abundances of volatiles and genetic relationships among submarine basalts from the Woodlark Basin, southwest Pacific. Geochim. Cosmochim. Acta 55, 2231–2239.

Pearce, J.A., Stern, R.J., 2006. The origin of back-arc basin magmas: trace element and isotopic perspectives. In: Christie, D.M., Fisher, C.R., Lee, S.-M., Givens, S. (Eds.), Back-Arc Spreading Systems: Geological, Biological, Chemical, and Physical Interactions. AGU monograph 166, Washington DC, pp. 63–86.

Perfit, M.R., Langmuir, C.H., Chappell, M.B., Johnson, R.W., Staudigel, H., Taylor, S.R., 1987. Geochemistry and petrology of volcanic rocks from the Woodlark Basin: addressing questions of ridge subduction. In: Taylor, Exon (Eds.), Marine Geology, Geophysics, and Geochemistry of the Woodlark Basin — Solomon Islands. Circum-Pacific Council for Energy and Mineral Resources, vol. 7, pp. 113–154.

Petterson, M.G., Neal, C.R., Mahone, J.J., Kroenke, L.W., Saunders, A.D., Babbs, T.L., Duncan, R.A., Tolia, D., McGrail, B., 1997. Structure and deformation of north and central Malaita, Solomon Islands: tectonic implications for the Ontong Java Plateau-Solomon arc collision, and for the fate of oceanic plateaus. Tectonophys 283, 1–33.

Petterson, M.G., Babbs, T., Neal, C.R., Mahoney, J.J., Saunders, A.D., Duncan, R.A., Tolia, D., Magu, R., Qopoto, C., Mahoa, H., Natogga, D., 1999. Geological–tectonic framework of Solomon Islands, SW Pacific: crustal accretion and growth within an intra-oceanic setting. Tectonophys 301, 35–60.

Ramsay, W.R.H., Crawfor, A.J., Foden, J.D., 1984. Field setting, mineralogy, chemistry, and genesis of arc picrites, New Georgia, Solomon Islands. Contrib. Mineral. Petrol. 88, 386–402.

Schuth, S., Rohrbach, A., Munker, C., Ballhaus, C., Garbe-Schonberg, D., Qopoto, C., 2004. Geochemical constraints on the petrogenesis of arc picrites and basalts, New Georgia Group, Solomon Islands. Contrib. Mineral. Petrol. 148, 288–304.

Sinton, J.M., Fryer, P., 1987. Mariana Trough lavas from 18°N: implications for the origin of back arc basin basalts. J. Geophys. Res. 92, 12,782–12,802.

Sinton, J.M., Ford, L.L., Chappell, B., McCulloch, M.T., 2003. Magma genesis and mantle heterogeneity in the Manus Back-arc basin, Papua New Guinea. Jour. Petrol. 44, 159–195.

Solomon, M., 1990. Subduction, arc reversal, and the origin of porphyry copper–gold deposits in island arcs. Geology 18, 630–633.

Staudigel, H., McCulloch, M., Zindler, A., Perfit, M., 1987. Complex ridge subduction and island arc magmatism: an isotopic study of the New Georgia forearc and the Woodlark Basin. In: Taylor, Exon (Eds.), Marine Geology, Geophysics, and Geochemistry of the Woodlark Basin — Solomon Islands. Circum-Pacific Council for Energy and Mineral Resources, vol. 7, pp. 227–240.

Stern, R.J., Lin, P., Morris, J.D., Jackson, M.C., Fryer, P., Bloomer, S., Ito, E., 1990. Enriched back-arc basin basalts from the northern Mariana trough: implications for the magmatic evolution of back-arc basins. Earth Planet. Sci. Lett. 100, 210–225.

Sun, S.-S., McDonough, W.F., 1989. Chemical and isotopic systematics of oceanic basalts: implications for mantle composition and process. In: Saunders, A.D., Norry, M.J. (Eds.), Magmatism in the ocean basins. Geol. Soc. London, Spec. Pub. , pp. 313–345.

Taylor, B., 1987. A geophysical survey of the Woodlark–Solomons Region. In: Taylor, Exon (Eds.), Marine Geology, Geophysics, and Geochemistry of the Woodlark Basin — Solomon Islands. Circum-Pacific Council for Energy and Mineral Resources, vol. 7, pp. 25–48.

Taylor, B., Martinez, F., 2003. Back-arc basin basalt systematics. Earth Planet. Sci. Lett. 210, 481–497.

Taylor, F.W., Mann, P., Bevis, M.G., Edwards, R.L., Cheng, H., Cutler, K.B., Gray, S.C., Burr, G.S., Beck, J.W., Phillips, D.A., Cabioch, G., Recy, J., 2005. Rapid forearc uplift and subsidence caused by impinging bathymetric features: examples from the New Hebrides and Solomon arcs. Tectonics 24, TC6005. doi:10.1029/2004TC001650.

Thorkelson, D.J., 1996. Subduction of diverging plates and the principles of slab window formation. Tectonophysics 255, 47–63.

Thorkelson, D.J., Breitsprecher, K., 2005. Partial melting of slab window margins: genesis of adakitic and non-adakitic magmas. Lithos 79, 25–41.

Trull, T.W., Perfit, M.R., Kurz, M.D., 1990. He and Sr isotopic constraints on subduction contributions to Woodlark Basin volcanism, Solomon Islands. Geochim. Cosmochim. Acta 54, 441–453.

Weissel, J.K., Taylor, B., Karner, G.D., 1982. The opening of the Woodlark Basin, subduction of the Woodlark spreading system, and the evolution of northern Melanesia since mid-Pliocene time. Tectonophys 87, 253–277.

Yoneshima, S., Mochizuki, K., Araki, E., Hino, R., Shinohara, M., Suyehiro, K., 2005. Subduction of the Woodlark Basin at New Britain Trench, Solomon Islands region. Tectonophys 397, 225–239.